CORROSION SCIENCE AND TECHNOLOGY, Vol.2, No.6(2003), pp.266~271

Advanced Indentation Studies on the Effects of Hydrogen Attack on Tensile Property Degradation of Heat-Resistant Steel Heat-Affected Zones

Yeol Choi, Jae-il Jang, Yun-Hee Lee*, Dongil Kwon*, and Jeong-Tae Kim**

Frontics, Inc., Seoul 151-742, KOREA
**School of Materials Science and Engineering*
Seoul National University, Seoul 151-742, KOREA
***R&D center, Doosan Heavy Industries & Construction Co., LTD.*
Changwon 641-792, KOREA

Safety diagnosis of various structural components and facilities is indispensable for preventing catastrophic failure of material by time-dependent and environment accelerating degradation. Also, this diagnosis of operating components should be done periodically for safe maintenance and economical repair. However, conventional standard methods for mechanical properties have the problems of bulky specimen, destructive procedure and complex procedure of specimen sampling. So, a non-destructive and simple mechanical testing method using small specimen is needed. Therefore, an advanced indentation technique was developed as a potential method for non-destructive testing of in-field structures. This technique measures indentation load-depth curve during indentation and analyzes the mechanical properties related to deformation such as yield strength, tensile strength and work-hardening index. In this paper, we characterized the tensile properties including yield and tensile strengths of the V-modified Cr-Mo steels in petro-chemical and thermo-electrical plants. And also, the effects of hydrogen-assisted degradation of the V-modified Cr-Mo steels were analyzed in terms of work-hardening index and yield ratio.

Keywords : *advanced indentation test, V-modified Cr-Mo steels, work-hardening index, yield ratio, hydrogen attack, HAZ, degradation*

1. Introduction

1.1 Research background

With viewpoints of failure prevention and lifetime extension, the evaluation of the structural integrity in welded joints has been one of the key issues recently. Therefore, the reliability assessment of weldment by mechanical tests including strength and fracture mechanics tests has become general practice throughout the world, because the welded joint having the microstructural and mechanical inhomogeneities[1),2)] is well known as the weakest regions in the structures. For example, the petrochemical refinery industry needs a long-term operation of the reactor at high temperature and hydrogen pressure. This severe environment can cause various degradation damages such as temper embrittlement and hydrogen-assisted degradation.[3)-5)] To satisfy the resistance to creep and hydrogen attack, Cr-Mo-V steel is used and this reactor structure was made by welding process. But, welded structure in hydrogen environment was degraded by surface decarburization and bubble formation at grain boundary.[6)] Especially, heat affected zone was more sensitive to hydrogen than base metal. Therefore, proper evaluation of this part is needed for safe operation of reactor. However, conventional standard tests such as the uniaxial tensile and the fracture mechanics tests, which need the specimen size requirement and complex testing procedures, cannot be easily applied to the testing of local regions such as welded joint. Until now, the direct evaluation of mechanical properties of welded joint has been mainly limited to the measurement of micro-Vickers hardness. To overcome the limitation of the conventional test, the need for new mechanical testing method applicable to the local welded joint has been increased. And, an advanced indentation technique satisfies the needs.[7)]

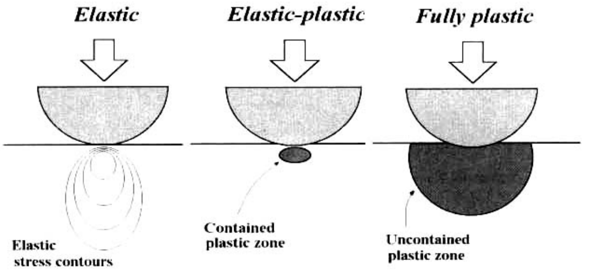

Fig. 1. Schematic diagram of mechanical deformation stages during a spherical indentation.

1.2 Evaluation of mechanical strengths using advanced indentation technique

The advanced indentation technique is developed from the conventional hardness test. This technique measures the indentation load and penetration depth during loading and unloading by spherical indenter at a constant speed, instead of the direct observation and measurement of indent size in the conventional hardness test. An indentation load-depth curve is obtained from this procedure similar with the load-displacement curve from the uniaxial tensile test. This curve represents the deformation behavior of testing sample beneath the rigid ball indenter.[8] The equivalent true stress and strain identical with the flow properties from the standard uniaxial tensile test can be predicted from the analysis of indentation load-depth curve considering the indentation stress fields and deformation shape.[9]

In this paper, authors simulated the microstructure of HAZ at Cr-Mo-V steels and characterized the mechanical properties using new advanced indentation technique. As the spherical indenter penetrates into material, mechanical deformation is divided as three stages of elastic, elastic/plastic, fully plastic as shown in Fig. 1.[10]

A reversible deformation occurs at low load indentation. When the indentation stress fields satisfy the yield criterion, plastic zone occurs inside the material and expands to free surface. And, the contact mean pressure beneath the spherical indenter rapidly increases in this elastic/plastic region. Finally, the expanded hemi-spherical plastic zone grows into the surrounding elastic zone with a constant velocity as the indentation depth increases. The contact mean pressure slightly increases in this fully plastic region. These deformation stages are similar to the work-hardening behavior of the uniaxial tensile test.

Researches for predicting the uniaxial flow properties from indentation-induced deformation were done as below. The raw data from the advanced indentation test is the indentation load-depth curve as shown in Fig. 2. The equivalent stress and strain were defined in terms of the measured indentation contact parameters such as contact depth, h_c*, indenter shape and the morphology of the deformed sample surface. And, real contact properties were determined by considering both the elastic deflection and the material pile-up around the contacting indenter as shown in Fig. 3.

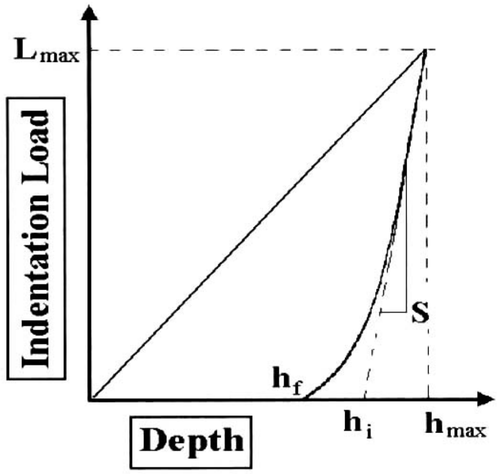

Fig. 2. Schematic of the indentation load-depth curve.

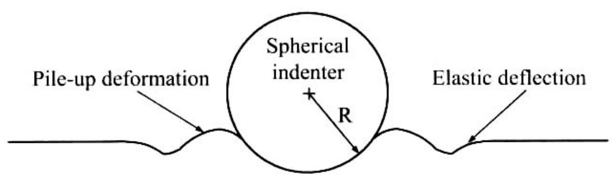

Fig. 3. Schematics of elastic and plastic deformation around indenter.

Firstly, a contact depth at maximum indentation load can be evaluated by analyzing the unloading curve with the concept of indenter geometry and elastic deflection as shown in Eq. (1).[11]

$$h_c^* = h_{max} - w\,(h_{max} - h_i) \qquad (1)$$

hi is the intercept indentation depth as shown in Fig. 2 and indenter shape parameter, ω is 0.75 for the spherical indenter. Secondly, the material pile-up around indentation enlarges the contact radius from the analysis of elastic deflection. The extent of this pile-up is determined by a constant c and work-hardening index, n for steels in Eq. (2).[12),13]

$$c^2 = \frac{a^2}{a^{*2}} = \frac{5(2-n)}{2(4+n)} \quad (2)$$

where, a is the real contact radius and a* is the contact radius without considering the pile-up around indent. Using the geometrical relationship of the spherical indenter, the real contact radius is expressed as Eq. (3) in terms of indenter radius, R and h_c*.

$$a^2 = \frac{5(2-n)}{2(4+n)}(2Rh_c^* - h_c^{*2}) \quad (3)$$

The contact mean pressure, P_m is expressed as Eq. (4).

$$P_m = \frac{L_{max}}{\pi a^2} \quad (4)$$

An equivalent strain, ε_R of indentation is evaluated from the material displacement beneath the indenter along the indentation axis direction. The equivalent strain is expressed in Eq. (5) at the position of the contact radius by multiplying a fitting constant α. The value of α is used as 0.1 for various steels.[9)]

$$\varepsilon_R = \frac{\alpha}{\sqrt{1-(a/R)^2}}\frac{a}{R} \quad (5)$$

In the case of metals including structural steels, the elastic and elastic/plastic deformation stages occurred at very low indentation load. Therefore, we considered only the plastic deformation region in this study. The equivalent stress, σ_R can be evaluated using the relationship with contact mean pressure as shown Eq. (6).[10)]

$$\frac{P_m}{\sigma_R} = \Psi \quad (6)$$

Ψ is a constraint factor for plastic deformation and the upper limit is about 3 for fully plastic deformation of steels. The exact values of work-hardening index, equivalent stress and strain are calculated by iteration method.[9)]

From the analysis of each unloading curve, both equivalent stress and strain values are determined. The stress and strain relation is fitted as the power-type Hollomon equation expressing work-hardening behavior. The fitted curve was extrapolated to initial yield and ultimate tensile regions. Then, yield strength was evaluated by inputting yield strain to Hollomon equation. And, ultimate tensile strength was evaluated using the concept that uniform elongation is equal to work-hardening index.

Table 1. Chemical compositions of 2.25Cr-1Mo-V steel.

Element(wt%)	C	Si	Mn	P	S	Ni	Cr	Mo	V
2.25Cr-1Mo-V	0.15	0.09	0.45	0.006	0.001	0.12	2.4	0.98	0.29

2. Experimental

Used material in this study is 2.25Cr-1Mo-V steel, whose chemical composition is listed in Table 1. Weld simulations were performed to investigate the change in tensile behavior of the heat-affected zones (HAZ) of the steel weldment with hydrogen exposure time. The specimens were thermally cycled in Thermicmaster system for simulating HAZ especially near fusion line, which are generally known as the weakest region among various regions of HAZ. After reaching 1137 K, the specimens were held 3 sec and cooled down with the constant cooling time from 1073 K to 773 K of 60 seconds. The cooling rate was approximately equivalent to those of a tandem SAW (submerged arc welding) with heat input of 27 kJ/cm in a 25-mm-thick-plate. The simulated HAZ specimens did experience post-weld-heat-treatment at 963 K for 24 hours, and then were exposed at 873 K in hydrogen pressure of 54 MPa for 408 and 1000 hours to evaluate the tensile property change with increasing hydrogen exposure time. The specimens exposed in hydrogen pressure were compared with the specimen without hydrogen exposure.

Testing system used for advanced indentation test was AIS2000, shown in Fig. 4, made by Frontics, Inc. The maximum indentation depth was 250 μm, and 15 partial unloadings down to 50% of maximum load at each point were applied. All loading and unloading speed was 0.3 mm/min. The indentation load-depth curve obtained from the multiple indentation technique was analyzed as flow properties including yield strength, work-hardening index and ultimate tensile strength based on the theoretical background. In case of the simulated HAZ specimens, the tests were done for the small regions in the simulated specimens as shown in Fig. 5 using WC ball indenter of 0.5 mm radius. Generally, the testing modes for true stress-strain relationship can be selected as maximum load and maximum depth controlling methods. In this study, maximum depth controlling mode for same equivalent strain was used.

3. Results and discussion

Indentation load-depth curves for various hydrogen-attacked specimens are shown in Fig. 6. The indentation load increased with increasing the hydrogen exposure time

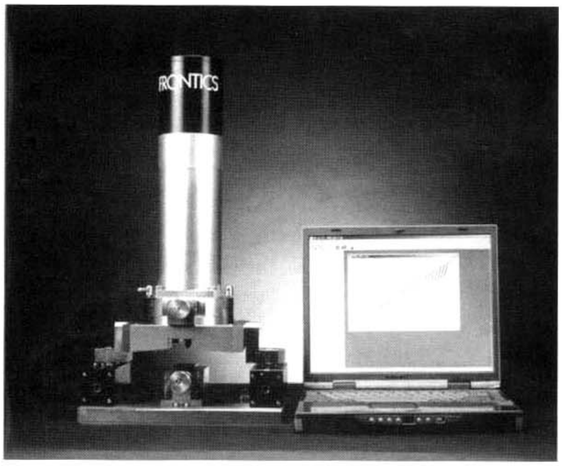

Fig. 4. Advanced indentation system (developed by Frontics, Inc.).

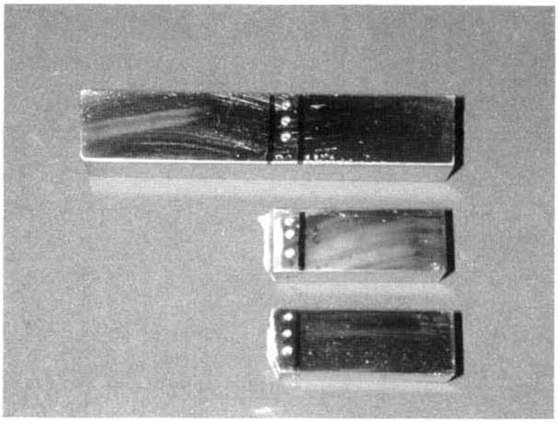

Fig. 5. Actual view of the simulated specimens tested by advanced indentation technique

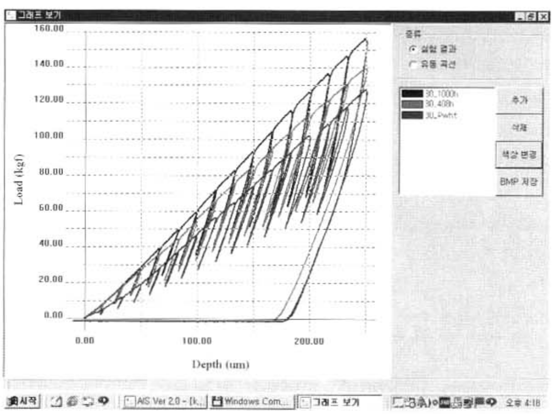

Fig. 6. The comparison of indentation load-depth curves with hydrogen exposure time in 2.25Cr-1Mo-V steel.

at a given maximum indentation depth. The behavior of material hardening with the exposure time can be predicted from Fig. 6. The hardening and embrittlement of the hydrogen-attacked material were reported by the formation of methane bubbles in grain boundary.[14)]

And, the true stress-strain curve analyzed from the indentation load-depth curve showed a same trend with the prediction in the raw testing result. The changes in yield and ultimate tensile strengths by the hydrogen-assisted degradation were plotted in Fig. 7. Yield strength increased significantly with the increase of the exposure time as shown in Fig. 7a. However, the change in ultimate tensile strength did not have any general trend with the hydrogen exposure time as shown in Fig. 7b. The diagnosis of the hydrogen-assisted degradation with only the change in mechanical strengths has some risks. Therefore, we investigated new degradation parameters from the variations in the true stress-strain curves.

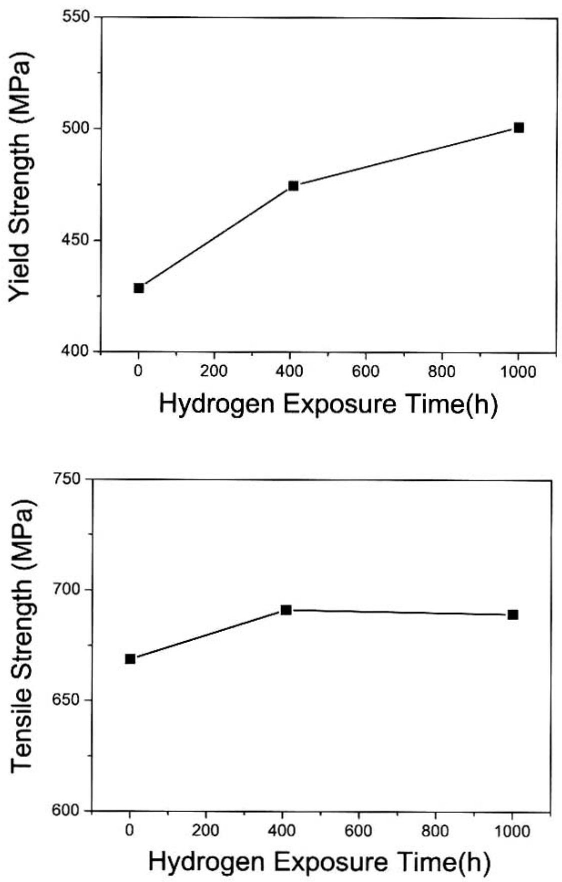

Fig. 7. The variation of mechanical properties with hydrogen exposure time; (a) yield strength, and (b) ultimate tensile strength in 2.25Cr-1Mo-V steel.

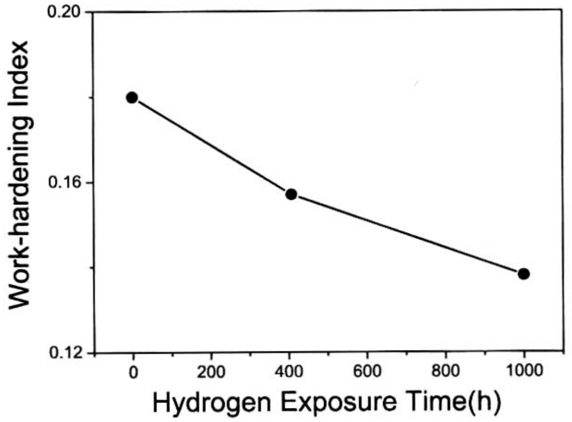

Fig. 8. The variation of work-hardening index with hydrogen exposure time in 2.25Cr-1Mo-V steel.

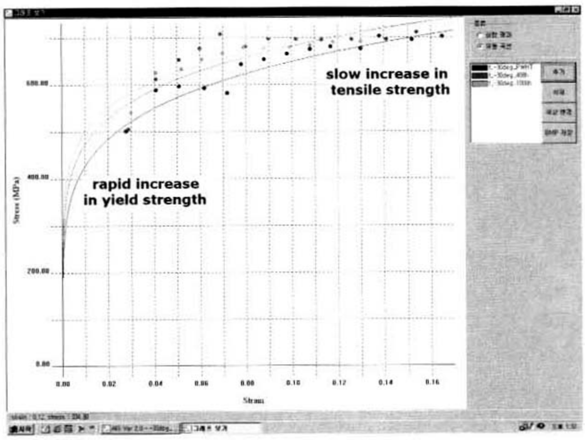

Fig. 9. The variation of yield and ultimate tensile strengths with increasing the hydrogen exposure time.

The variation of work-hardening index was surveyed in Fig. 8. A significant decrease with the exposure time was identified. Generally, work-hardening index of uniform material is proportional to uniform elongation. The reduction of work-hardening index means the embrittlement by hydrogen attack. But, work-hardening index is not regulated as an industrial specification for new material. So, the use of work-hardening index is not practical for in-field structures.

Therefore, we proposed another degradation parameter expressing the possibility of material deformation. The extents of variations in yield and ultimate tensile strengths were different as shown in Fig. 9. So, the ratio of yield to ultimate tensile strengths was varied with the hydrogen exposure time as shown in Fig. 10. Yield ratio significantly increased with the increase of the hydrogen exposure time.

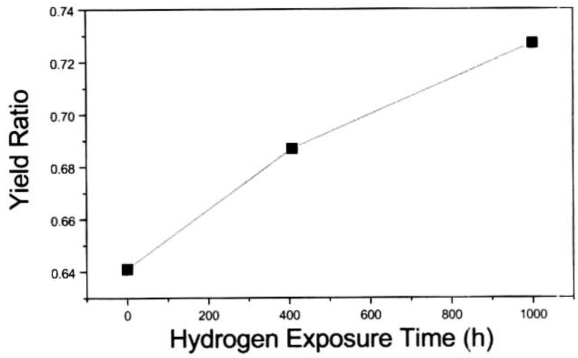

Fig. 10. The variation of yield ratio with hydrogen exposure time in 2.25Cr-1Mo-V steel.

And, the behavior of yield ratio was inverse proportional to that of work-hardening index or uniform elongation. This parameter showed a distinct change by the material degradation compared with other strength parameters. Also, the information for yield and tensile strengths is well known for new material. Therefore, the exact diagnosis of material degradation will be possible with the aids of this degradation parameter and advanced indentation technique.

4. Conclusions

The properties changes by hydrogen attack were investigated using the nondestructive advanced indentation test for the simulated HAZ in 2.25Cr-1Mo-V steel. The variations of yield and ultimate tensile strengths with increasing the hydrogen exposure time were tested. And, work-hardening index and yield ratio were proposed as indentation parameters to evaluate the material degradation by hydrogen. The major conclusions of this study are as follows:

(1) The indentation load-depth curves for the hydrogen-attacked material were obtained from the advanced indentation technique under the condition of a given maximum indentation depth. The indentation load increased with increasing the hydrogen exposure time. And, this result showed the hardening by material degradation.

(2) The change in the true stress-strain curve was investigated with increasing the hydrogen exposure time. Yield strength significantly increased by hydrogen attack. However, the variation of ultimate tensile strength was negligible and had no trend.

(3) Work-hardening index and yield ratio were proposed as indentation parameters to evaluate the degree of hydrogen attack. Yield ratio increased severely with increasing the exposure time. And, the potential of yield ratio as a degradation parameter was identified from the

experimental results.

References

1. S. Lee, B. C. Kim, and D. Kwon, *Metallurgical Transactions*, **23A**, 2803 (1992).
2. J.-B. Ju, J.-I. Jang, W.-S. Kim, and D. Kwon, in *Proceeding of 2000 International Pipeline Conference*, Canada, Vol.1, 169 (2000).
3. W. E. Erwin and J. G. Kerr, *WRC 275*, Feb., 158 (1982).
4. T. Kushda, J. Furusawa, Y. Shida, and T. Kudo, *ISIJ*, **73**, 1778 (1987).
5. H. Okada and K. Naito, in *1st Int. Conf. Proceedings on Current Solutions to Hydrogen Problem in Steels*, ASM, Nov. (1982).
6. American Petroleum Institute, Steels for Hydrogen Service at Elevated Temperature and Pressure in Petroleum refineries and Petrochemical Plants, API Publication 941, 2nd Edition, June (1977).
7. Y.-H. Lee, Y. Choi, J.-H. Ahn, D. Kwon, and J. S. Cheon, in *Transactions of the 15th International Conference on Structural Mechanics in Reactor Technology*, III 277 (1999).
8. J. S. Field and M. Swian, *Journal of Materials Research*, **10**, 101 (1995).
9. J.-H. Ahn, Y. Choi, and D. Kwon, *Journal of the Korean Institute of Metal and Materials*, **38**, 1606 (2000).
10. F. A. Francis, *Journal of Engineering Materials and Technology, Transaction ASME*, **98**, 272 (1978).
11. W. C. Oliver and G. M. Pharr, *Journal of Materials Research*, **7**, 1564 (1992).
12. A. L. Norbury and T. Samuel, *Journal of Iron and Steel Institute*, **117**, 673 (1928).
13. R. Hill, B. Storåkers, and A. B. Zdunek, *Proceedings of Royal Society in London*, **A423**, 301 (1989).
14. D.-J. Kim, B.-H. Kim, B.-O. Kong, J.-T. Kim, Y.-H. Kwon, H.-S. Park, and C.Y. Kang, *Journal of the Korean Welding Society*, **18**, 232 (2000).